FEMS Microbiology Ecology, 2025, 101, fiaf117
DOI: 10.1093/femsec/fiaf117
Advance access publication date: 26 November 2025
Research Article

Totivirus–satellite coinfection prevalence and host genotype associations in wild *Saccharomyces cerevisiae*

Tommy J. Travers-Cook[1,2,3,*], Sarah J. Knight[4], Soon Lee[4], Jana Jucker[2], Tamara Schlegel[1,2], Jukka Jokela[1,2], Claudia C. Buser[1,4,5]

[1]Institute of Integrative Biology, ETH Zürich, Zürich 8092, Switzerland
[2]Department of Aquatic Ecology, EAWAG, Dübendorf 8600, Switzerland
[3]Department of Zoology, University of British Columbia, Vancouver 4200, Canada
[4]School of Biological Sciences, University of Auckland, Auckland 1010, New Zealand
[5]Institute of STEM Education, St. Gallen University of Teacher Education, St. Gallen 9000, Switzerland
*Corresponding author. Institute of Integrative Biology, ETH Zürich, Zürich 8092, Switzerland. Email: tommy.traverscook@zoology.ubc.ca
Editor:: Ville-Petri Friman

Abstract

Saccharomyces cerevisiae is occasionally infected by dsRNA totiviruses and their toxin-encoding dsRNA satellite nucleic acids. The autonomous totivirus and its satellite can coexist but with an asymmetric dependence of the satellite on the totivirus for replication and maintenance inside the host cell. Satellites provide their yeast hosts with inhibitory toxins and the necessary self-immunity; loss of the satellite equates to loss of toxin immunity. Because these viral elements lack known extracellular stages, and sex is suspected to be rare, they are assumed to be transmitted vertically, implying that infection states should correlate with host genotypes. However, totivirus–satellite coinfections are rarely examined in natural populations, leaving their associations with host genotypes poorly understood. We screened a multiyear, vineyard-associated population of *S. cerevisiae* isolates from New Zealand to examine the stability of host–virus associations over time, both within and across genotypes. Over half of the wild isolates harbored infections (55%), but less than half of these (37% of infected) had toxin-encoding satellites. Genotypes that persisted across years typically maintained consistent infection states. However, we also observed stepwise transitions from coinfection through infection to an infection-free state, as well as acquisition of totiviruses and satellites. Genotypes clustered strongly by infection state, and population heterozygosity was significantly lower than expected, supporting vertical transmission while suggesting that outcrossing is not responsible for the acquisition of higher infection states. Despite occasional intragenotypic transitions, genotype clustering by infection state remained intact, suggesting that such transitions are transient and that host genotypes may have optimal infection states with regard to totiviruses and their satellites.

Keywords: coevolution; ecological genetics; killer yeast; mycoviruses; sexual reproduction; transmission mode

Introduction

Mycoviruses, those that infect fungi, tend not to cause overt harm or disease-like symptoms for their fungal hosts (Ghabrial et al. 2015). Mycoviral infections tend to be chronic and nonlytic, whereby transmission is generally restricted to vertical transmission from parent to progeny (Ghabrial and Suzuki 2009, Ghabrial et al. 2015, Buivydaite et al. 2024). An intrinsic consequence of vertical transmission is selection for benignity to prevent host mortality (Anderson and May 1982, Bull 1994, Messenger et al. 1999, Alizon et al. 2009). The fitness of both host and mycoviruses therefore tend to be coupled and enforced through partner fidelity feedbacks (Ewald 1987, Doebeli and Knowlton 1998, Herre et al. 1999, Sachs et al. 2011). Many fungi are facultatively sexual, reproducing mostly through clonal reproduction and intratetrad mating, while still undergoing sexual cycles that can facilitate the spread of mycoviruses (Bennett and Turgeon 2016, Nieuwenhuis and James 2016). Mycoviruses are therefore believed to diverge with host genotypes, which is supported by observations over macroevolutionary time (Goker et al. 2011).

Saccharomyces cerevisiae often harbours mycoviruses, typically of a dsRNA variety (Wickner et al. 2013, Wickner 1996a). The most well-studied of these is the monopartite dsRNA totivirus (family Totiviridae), which on occasion is found to coinfect *S. cerevisiae* with a separately encapsidated monopartite dsRNA satellite nucleic acid (Magliani et al. 1997, Schmitt and Breinig 2002, 2006). Totiviruses are believed to reside permanently in the host cell, and replicate autonomously, due to their possession of two overlapping open reading frames (ORFs) enabling encapsidation and replication (Icho and Wickner 1989, Dinman et al. 1991, Fujimura et al. 1992, Dinman and Wickner 1994). Satellite nucleic acids of totiviruses are obligatorily dependent on the machinery and resources of totiviruses (Bostian et al. 1980). However, the satellite's single ORF encodes a preprotoxin—an unprocessed precursor of a mature, secretable toxin—which also encodes functional immunity for the host (Hanes et al. 1986, Dignard et al. 1991, Schmitt and Tipper 1995).

The secreted killer toxin can be lethal to competitors of the host strain that do not possess the same totivirus–satellite coinfection type or have evolved resistance (Hanes et al. 1986). Satellite-

Received 5 May 2025; **revised** 17 November 2025; **accepted** 17 November 2025

encoded toxins are generally believed to be used by *S. cerevisiae* as an interference competition strategy for invading novel environments or for preventing invasions by distantly related genotypes lacking the coinfection (Boynton 2019, Travers-Cook et al. 2023). It has also been proposed that satellite-encoded toxin production acts analogously to toxin–antitoxin systems in bacteria (Kast et al. 2015, Wickner and Edskes 2015, Jurenas et al. 2022), whereby loss of the satellite nucleic acid leads to immediate competitive exclusion by clonal neighbours that maintain their toxin-encoding coinfection.

The totivirus–satellite association may be best considered under the context-dependent mutualism framework (Bronstein 1994). There is an asymmetric dependence of the satellite on the totivirus. Unlike many mycoviruses, the totivirus detriments host fitness by inducing proteostatic stress at high temperature under laboratory conditions (Chau et al. 2023). The satellite hijacks capsid proteins and polymerases for its own replication, which may slow the totivirus replication rate or encourage selection for virulent mutants of the totivirus (Bostian et al. 1980, Taylor et al. 2014). While there may be selection on totiviruses to suppress resource hijacking by the satellite, removal of the satellite can result in host toxin sensitivity and mortality by the actions of clonal neighbours (Woods and Bevan 1968, Marquina et al. 2002). Depending on density-dependence and the frequency of toxin-based interference competition, this may prevent yeast without satellite infections from fixing (Wickner and Edskes 2015). *Saccharomyces cerevisiae* has mechanisms in place to suppress totivirus proliferation, which are most effective against coevolved totiviruses whom they have adaptations in place for (Rowley et al. 2016, Gao et al. 2019). *Saccharomyces cerevisiae* can be cured of the satellite with relative ease under high temperature treatments (Wickner 1974). The bias of vertical transmission of totivirus–satellite coinfections has selected for them to have minimal impact on host gene expression, demonstrated during artificial infection-curing experiments (McBride et al. 2013, Luksa et al. 2017). This is however limited to those that have a coevolved history with their hosts, as introduction of novel satellites results in decreased fitness relative to when host are reinfected with the coevolved satellites (Pieczynska et al. 2017).

It is not known whether infections are stable and consistent within host genotypes in natural populations of *S. cerevisiae*. Beyond cytoplasmic conflict between totiviruses and their satellites, rare sexual events may mix host–virus–satellite lineages and perhaps result in progeny having different mycoviral infections than those of their parents. Though sexual reproduction is considered to infrequently occur (Bennett and Turgeon 2016, Nieuwenhuis and James 2016), it is the suspected explanation for the occasional mismatching of totivirus–satellite combinations from their native pairings (Quintero-Blanco et al. 2022). Killer phenotype bearing strains from broad geographic origins have been found to be somewhat phylogenetically clustered within nonkiller strains, yet killer phenotypes are evidently gained and lost (Pieczynska et al. 2013). Yeast isolates from the same sampling sites over time have rarely been screened for totivirus–satellite coinfections (Starmer et al. 1987), such that the frequency, or infrequency, of gains and losses of *S. cerevisiae*'s mycoviruses in wild populations is not well studied. It is undetermined whether infection states diverge with their host genotypes, or whether host–virus–satellite conflict and sexual reproduction are processes capable of distorting associations between host genotype and infection status.

In this paper, we utilize a multiyear collection of cooccurring vineyard-associated *S. cerevisiae* isolates from across New Zealand covering years 2018, 2019, and 2021, to explore the prevalence and persistence of totivirus–satellite (co)infections in natural populations of *S. cerevisiae*. To do so, we quantify the prevalence of the different infection states in this vineyard-associated population and codivergence of infection state with the host genotype. We also examine the frequency of genotype-level transitions in infection state and whether these transitions disrupt associations between host genotypes and infection status.

Materials and methods

Yeast sample isolation

We studied a collection of *S. cerevisiae* isolates from vineyards across the Hawke's Bay and Marlborough regions of New Zealand. Yeast isolates were sampled in 2018, 2019, and 2021 from a set of 25 vineyards (Table S1). Grape varieties at each vineyard belonged to either Merlot, Pinot Noir, or Sauvignon Blanc (Table S1).

Fruit was collected 1–3 days prior to the commercial harvest. For Sauvignon blanc, whole bunches were hand harvested from vines using sterile snips from nine random locations within each vineyard block, totaling 40 kg of fruit from each vineyard site. For each vineyard site, the fruit was crushed and destemmed mechanically under carbon dioxide (CO_2) cover and 30 ppm of SO_2 (potassium metabisulfite) was added to the must. The must was chilled at 6°C for 1 h on skins before being pressed in a balloon press at 2 bar for 3 min and 4 bar for 14 min. The pressed juice was left to cold settle overnight at 6°C before being racked off lees under CO_2 cover into 18 l fermentation vessels. Lees were added back to adjust turbidity to between 150 and 200 nephelometric turbidity units. The juice was warmed to 16°C for uninoculated fermentation. Fermentation was performed at and monitored by weight loss (El Haloui et al. 1988). Once fermentation began (weight loss of >100 g in 24 h) a standard complex nutrient addition of 600 ppm (0.6 g/l) Nutristart® (Laffort®, Bordeaux, France) was added. Fermentation was considered complete when no weight was lost for two consecutive days and the residual sugar concentration was <2 g/l as determined by AimTab™ reducing substances tablets (Germaine Laboratories Inc., San Antonio, TX, USA). Postfermentation, a 1 ml sample was taken and stored in 15% glycerol at −80°C whilst awaiting processing. All equipment was washed with water and sanitized with 70% ethanol between samples.

For red wines (Merlot and Pinot Noir), whole bunches were hand harvested in the same manner to a total of 17 kg per site. The fruit was destemmed by hand under CO_2 cover and 15 ppm of SO_2 (PMS) was added to the must. The must was cold soaked at 6°C for 3 days and the cap (grape skins, pulp, and stems) was submerged twice during this time. If the pH was >3.6, tartaric acid was added to drop it below this level. It was then warmed to 25°C for uninoculated fermentation and monitored during fermentation to ensure the temperature peaked between 28°C and 32°C. As with the Sauvignon Blanc fermentation, 600 ppm (0.6 g/l) Nutristart® (Laffort®) was added as fermentation began. During the course of fermentation, the cap was manually plunged once daily and it was deemed complete once the sugar level dropped below 2 g/l as determined by AimTab™ reducing substances tablet (Germaine Laboratories Inc.). A 1 ml sample for microbial analysis was taken postfermentation and before the wines were pressed from each wine and stored in 15% glycerol for later analysis.

Identification of *S. cerevisiae*

Ferment samples were serially diluted onto standard YPD agar plates (1% yeast extract, 2% peptone, 2% dextrose, and 2% agar

powder) and incubated for 2 days at 20°C. Afterwards, 96 colonies were picked from each sample for further analysis. Genomic DNA was extracted by incubating colonies at 37°C for 30 min in a pH 7.5 20 µl solution of 1.25 mg/ml zymolyase dissolved in 1.2 M sorbitol and 0.1 M KH_2PO_4 followed by 10 min of incubation at 95°C. A multiplex Polymerase Chain Reaction (PCR) was used to confirm that the yeast isolates belonged to *S. cerevisiae* or *S. uvarum* (de Melo Pereira et al. 2010). The SacScreen PCR reaction contained 1x KAPA 2 G Readymix (Kapa Biosystems, Wilmington, MA, USA), 0.4 µmol/l of each SacScreen primer (Pereira et al. 2010), ∼10 ng DNA template and H_2O to a total volume of 10 µl per reaction. The SacScreen PCR settings were as follows: an initial denaturing step of 95°C for 3 min, followed by 35 cycles of denaturation (94°C for 30 s), annealing (55°C for 30 s), and extension (72°C for 2 min), all of which was concluded with a final extension step at 72°C for 5 min (Nadai et al. 2018). Products of the SacScreen PCR were visualized with gel electrophoresis to confirm membership as either *S. cerevisiae* or *S. uvarum*, all of which were *S. cerevisiae*.

Microsatellite genotyping and genotype assignment

Microsatellite markers were used to genotype eight colonies identified as *S. cerevisiae* per vineyard–year combination. A multiplex PCR was conducted for each *S. cerevisiae* colony, of which 10 µl reactions were made up of 5 µl QIAGEN Multiplex mastermix (Venlo, Netherlands), 1 µl of a 20-primer mixture (forward and reverse primers for nine informative microsatellite loci as well as primers for mating types), 2 µl genomic DNA and 2 µl H_2O (Richards et al. 2009). The PCR settings involved an initial denaturation step at 95°C for 15 min, followed by 35 cycles of denaturation (94°C for 30 s), annealing (55°C for 30 s), and extension (72°C for 2 min), concluded by a lengthened extension period (60°C for 6 min). PCR products were genotyped at Auckland Genomics on an Applied Biosystems (Waltham, Massachusetts, USA) 3130XL Genetic Analyzer. The ensuing trace files were analysed using the Geneious bioinformatics platform (Biomatters, Auckland, New Zealand). Of the nine microsatellite loci that isolates were initially scored for, eight are used in the analyses hereafter (Table S2). The YBR240C marker was excluded because it often had too many peaks on the trace files. The mating type (MATa and MATα) loci were amplified, yielding one peak in haploid isolates and two peaks in diploid isolates; all isolates were found to have two peaks.

Much of our analyses described hereafter were conducted with a refined dataset with complete microsatellite data because some of the methods used here do not handle missing data well. We designed a conservative pipeline to assign genotypes with missing data at microsatellite loci to genotypes with more complete microsatellite profiles. We first assigned genotypes for those with complete microsatellite profiles over the eight microsatellite loci, then we iteratively assigned the other isolates to these genotypes based on whether their available data could be nested into the microsatellite profile of only one other genotype. If an isolate with missing microsatellite data could be assigned to multiple other more complete genotypes based on its available microsatellite data, it was considered to have an ambiguous genotype assignment and discarded from analyses that utilized genotype assignment or microsatellite information (discriminant analysis of principal components and Markov chain transition probabilities). If the isolate's available microsatellite profile was not a complete match with any of the previously defined genotypes, it was treated as a unique genotype, but again removed from analyses (discriminant analysis of principal components and Markov chain transition probabilities). Whilst this approach resulted in a number of isolates with ambiguous genotype assignments being excluded from analysis (14.9%), we could avoid inflating the number of multilocus genotypes that were present due to missing data, whilst maintaining the genotype distribution. With this approach, distinct genotypes may be clustered into a single genotype; however, this will occur only with closely related sister genotypes that have diverged only recently, given the high mutation rate of microsatellites. We established a genotype accumulation curve for the refined population without missing data and visually compared this to genotype accumulation curve achieved when including isolates with missing data. Each locus was randomly sampled 10 000 times to create the distribution. We also quantified the relationship between number of individuals sampled and the number of unique genotypes observed, with 95% confidence intervals (Chao et al. 2014, Hsieh et al. 2016).

dsRNA extraction and virus typing

To establish the viral infection state of each yeast isolate, dsRNA was extracted from each yeast isolate using a modified version of Crabtree et al. (2019), in which only a single wash buffer (1x STE; 16% EtOH) step was applied, as this could prevent the unnecessary loss of dsRNA. The dsRNA precipitate was dissolved in molecular grade water before visualization using agarose gel electrophoresis. The presence of the totivirus in the yeast isolates was confirmed by a band at ∼4.6–4.8 kb, whilst the presence of the toxin-encoding satellite was confirmed by a band at ∼1.6 kb. Where an absence of dsRNA bands was found across a whole set of extractions, extraction sets were repeated to eliminate the possibility of erroneous extractions being responsible for the observation of virus-free isolates. From this, each yeast isolate could be allocated to one of three infection state groups: 'Totivirus– satellite coinfections', 'Totivirus infections', and 'Infection-free'. These groups, defined by the numbers of bands observed from the gel electrophoresis, are unambiguous and discrete (Fig. S1). These three groups capture all possible combinations as satellites can only inhabit yeast when the totivirus accompanies it, and as expected, it was never observed to infect alone.

Temporal changes in the proportions of different infection states

To assess the effect of the *year* on the relative proportions of each infection state found, compositional analysis was conducted using a multinomial Dirichlet regression model (Douma and Weedon 2019). The Dirichlet distribution is ideal for modelling infection state proportions because it captures the negative correlations between infection states through the sum-to-one constraint. Within vineyards there were instances of infection types being absent. To overcome this technical problem for calculating test statistics we added a small value of 1×10^{-5} to each infection count before calculating the proportions. This transformation ensures that the proportions derived from the count data fit within the [0,1] limits of the Dirichlet regression model. The same value was added to the denominator as a normalization factor to ensure all proportions were within the [0,1] limits. In the model, *year* was treated as a fixed effect and *vineyard* as a random effect, utilizing the Dirichlet family to account for the compositional nature of the data. The model was implemented using the brms package in R (Bürkner 2017), employing 10 Monte Carlo Markov chains of 5000 iterations for parameter estimation, with the first 2500 iter-

ations serving as a burn-in period. A total of 67 vineyard × year combinations were analysed, accounting for variability amongst 25 vineyards.

Intragenotypic infection state transition probabilities

To explore the consistency of coinfections within individual genotypes over time, a discrete-time Markov chain (DTMC) was constructed. This excluded individuals with ambiguous genotype assignments (based on missing microsatellite data), and genotypes that were only observed in 1 year, resulting in a total of 28 genotypes with multiyear presences (24.4%) being used for the calculations of transition probabilities. Transition matrices were created for each genotype, capturing the changes in infection state from 1 year to the next. Transition probabilities were computed based on the prevalence of each genotype in the current and subsequent years. Transition matrices were then aggregated across genotypes and years and normalized to ensure that each row sums to one, making the probabilities comparable across infection states. Confidence intervals for the transition probabilities were calculated across data for individual genotype transition probabilities across pairs of states. All analyses were conducted using the R programming language (R Core Team 2023), and plotted with ggplot2 (Wickham 2011).

Discriminant analysis of principal components

Discriminant analysis of principal components (DAPC) was used to cluster individuals according to their multilocus microsatellite profiles and infection states (Jombart et al. 2010). DAPC reduces the dimensionality of the microsatellite dataset with principal component analysis, to which discriminant analysis partitions the between- and within-group variation component to maximize the between-group differences. Discriminant analysis therefore summarizes the between group genetic differentiation. We reduced the dataset to isolates that have complete microsatellite genotype at the eight microsatellite loci used, after our genotype assignment method described previously.

Three DAPC models were calculated to untangle the contributions of genotype frequency and variable infections within genotypes on how genotypes cluster by infection state, all with cross-validation to determine the number of principle components (PCs) that achieve the highest mean successful assignment (MSA) and lowest mean squared error (MSE). We first conducted the DAPC with all individuals with complete microsatellite profiles ($n = 414$), with infection state set as the prior; this approach makes genotype weighting proportional to their frequencies. For this model, retaining 26 PCs achieved the highest MSA (0.861) and lowest MSE (0.153). Next, we applied a clone correction to remove replicate isolates of the same genotype. The first clone correction of the population included all genotypes and their replicates with different infection states ($n = 98$); this method gives additional weight to genotypes that have variable infection states and was used to see how infection state transitions disrupt the MSA. The highest MSA (0.728) and lowest MSE (0.309) was found when 10 PCs were retained. Finally, we further refined the collection to include only genotypes that were not observed to have variable infection states across the collection ($n = 67$). The final approach removes the weighting bias introduced by genotypes that have multiple infection states across the collection and explores only genotypes with consistent infection states. This model had the highest MSA (0.902) and lowest MSE (0.162) when 12 PCs were retained.

Analysis of population heterozygosity

To infer the frequency of outcrossing in the population, we compared expected and observed heterozygosity and tested for significant differences using *t*-tests. Analyses were performed on the complete population, on clone-corrected genotypes with and without genotypes that experienced infection state transitions, and on each infection state subpopulation. Comparing the complete population to subpopulations allows us to assess whether outcrossing is restricted to within infection states or occurs more broadly across the population. In a facultatively sexual system, observed heterozygosity significantly lower than expected suggests clonality or intratetrad matings.

Results

In total, 536 diploid yeast colony isolates were microsatellite genotyped across 25 vineyards over 1–3 years. Prior to any form of genotype correction, 188 genotypes were identified. Correcting for ambiguous assignment by nesting isolates with missing data into more complete genotypes as described in the methods section, resulted in 119 genotypes and 80 individual isolates with ambiguous microsatellite genotype assignments (14.9%)—these isolates were excluded from analyses that required genotype information. Isolates with complete microsatellite profiles (eight loci) after our assignment method totaled to 414 individuals of 80 genotypes (77.2% of individual isolates). The decline from 119 to 80 genotypes is due to the presence of individuals with unique microsatellite profiles yet with missing data. The genotype accumulation curve demonstrates that the asymptote has not yet been reached for the number of loci needed to discriminate the individuals into genotypes and the number of individuals needed to get all the genotypes present for this number of microsatellite loci (Fig. S1).

Of the 536 isolates in the collection, we successfully established virus profiles for 534 individuals (99.6%). In summary, 240 were free of any form of cytosolic dsRNA (infection-free), 185 isolates possessed a gel band corresponding to the sole presence of totiviruses (totivirus infection) and 109 isolates possessed gel bands corresponding to the presence of the totivirus and its coinfecting satellite (totivirus–satellite coinfections; Fig. 1A). Less than half of isolates with the totivirus infection were observed to also have a toxin-encoding satellite (37.1%). Of the 119 MLGs identified, 28 MLGs appear in multiple years and 15 were found to have multiple viral profiles (Fig. 2).

Temporal changes in the proportions of different infection statuses

A multinomial Dirichlet regression model was employed to assess the effect of year on the relative proportions of different infection statuses across vineyards, with the infection-free group serving as the reference. The random effect of vineyard revealed moderate variability in infection type proportions across sites, with the standard deviation of the intercept for totivirus infections estimated at 0.33 (95% CI: [0.01, 0.81]) and for totivirus–satellite coinfections at 0.21 (95% CI: [0.01, 0.58]). This suggests greater vineyard-level variability in the prevalence of totivirus infections compared to totivirus–satellite coinfections.

Regression coefficients are reported on the log scale of the Dirichlet concentration parameters. Negative estimates indicate a lower expected proportion relative to the reference year (2018), and positive estimates indicate a higher expected proportion. Confidence intervals on this scale are not bounded between 0 and 1, while overlaps with 0 indicate uncertainty about whether

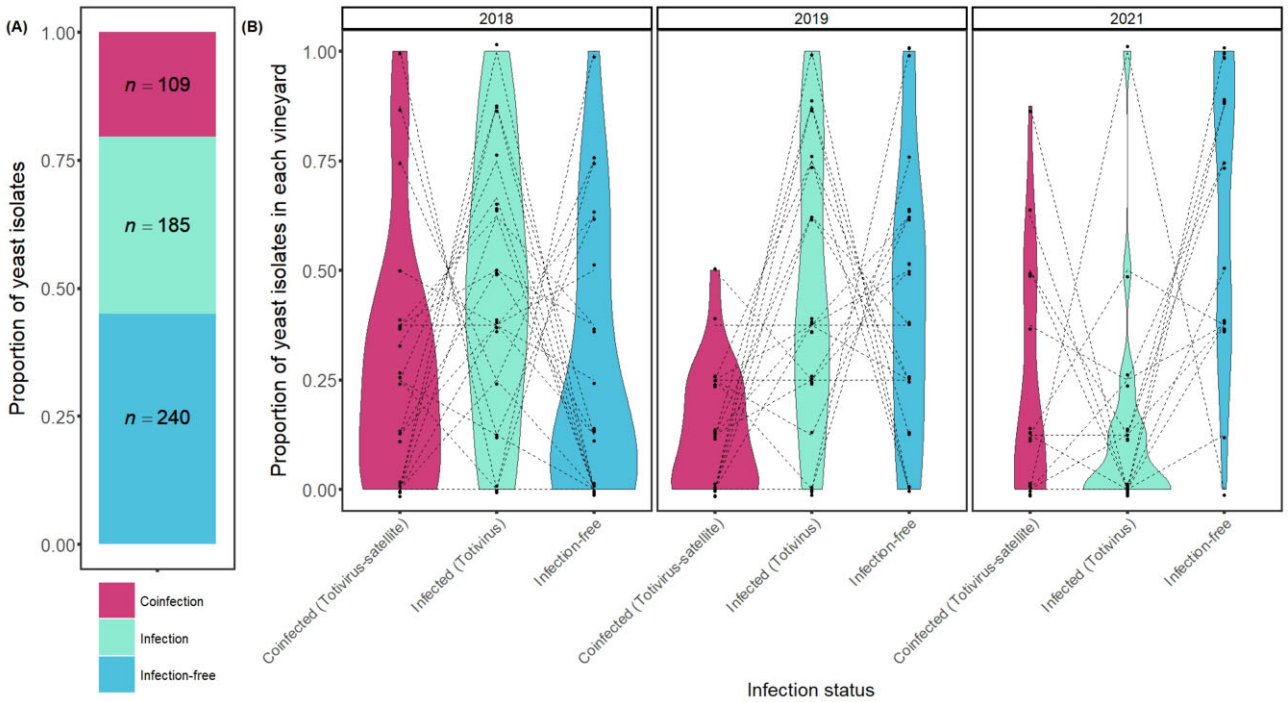

Figure 1. The proportions of each infection status in the population. (A) The overall proportions of each infection status in the population with the frequency (*n*) of each seen in each stack of the bar plot. (B) The proportions of each infection status across year in individual vineyards. Dotted lines connect proportions from the same vineyards and demonstrate that the proportions equal to 1.

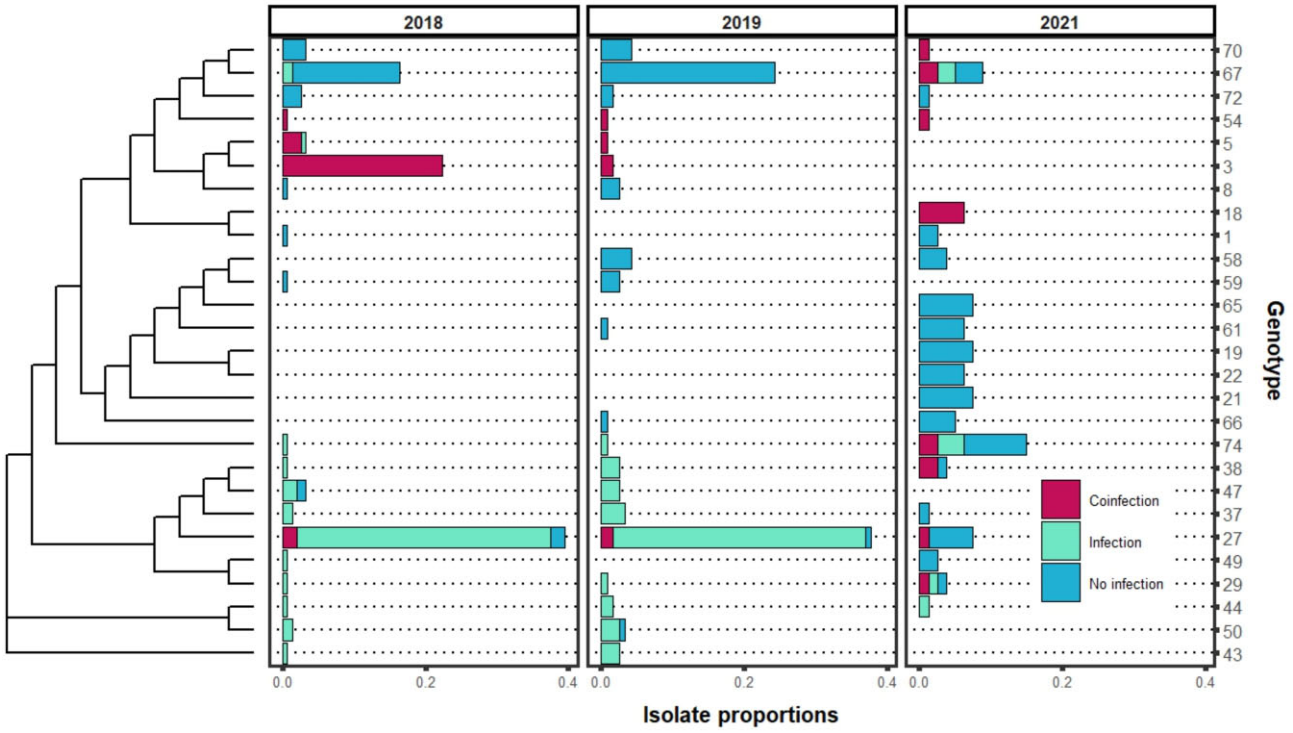

Figure 2. Neighbour-joining tree showing the relationships between microsatellite genotypes that appear ≥3 times in the collection, and the relative proportion of each genotype each year mapped on to the phylogeny.

the effect differs from the reference year. Relative to the reference year of 2018, totivirus infections had a moderately lower prevalence in 2019 (estimate: −0.60; 95% CI: [−1.39, 0.19]; Fig. 1B) and a substantially lower prevalence in 2021 (estimate: −1.88; 95% CI: [−2.72, −1.05]; Fig. 1B). Totivirus–satellite coinfections were also less prevalent in 2019 (estimate: −0.74; 95% CI: [−1.55, 0.09]; Fig. 1B) and in 2021 (estimate: −1.19; 95% CI: [−2.02, −0.36]; Fig. 1B).

Intragenotypic transition probabilities

The genotype infection state transition probability matrix indicates that if the same genotype was found in multiple years, it most likely maintained its infection status (diagonal, Fig. 3). There were, however, rare transitions to all of the other infection states (off-diagonal; Fig. 3). The transition matrices suggest that state transitions occur almost exclusively in a stepwise manner. Transition probabilities from coinfection to infection-free, and vice versa, were rarely observed, if at all (0–0.01; Fig. 3). Maintenance of a totivirus infection was most probable of all (0.822), and remaining infection-free was the most improbable (0.717) among the nontransitions. Nonetheless, transitions between all states were observed at least once, including gains of totiviruses and/or satellites (Fig. 3).

DAPC

To visualize how infection state interrelates with *S. cerevisiae* genotype, the results of the two linear discriminants of the DAPC were plotted with infection state as a prior, with the three previously defined approaches (Fig. 4). Using all individuals with full microsatellite profiles after our customized genotype assignment (Fig. 4A), we see strict clustering of individuals by their infection states. The first linear discriminant alone was capable of near-perfect discrimination of uninfected individuals from those with totivirus–satellite coinfections. The second discriminant was equally capable of discriminating totivirus-infected individuals from the other two groups. Infected isolates are at an intermediate level between coinfected isolates and uninfected isolates on the first linear discriminant. The coinfection virus profile is the most distinct of the three infection states, whilst infected and uninfected isolates cluster more frequently with each other.

This distribution of the various infection states over the two linear discriminants is also observed across the other two models, but with noticeable differences (Fig. 4B and C). For the clone-corrected genotypes including those with multiple infection states (Fig. 4B), all three infection state priors coalesce and overlap in the DAPC coordinate space of the infected isolates, such that the inertia ellipses of the coinfected and uninfected prior groups extend towards 0 and past it (towards negative values for uninfected group and towards positive values for the coinfected group) on the first linear discriminant and towards positive values on linear discriminant 2. Once the population is further refined to remove genotypes that were observed to have multiple infection states (Fig. 4C), we see the reemergence of distinct clusters, with some overlap between the totivirus-infected and uninfected isolate clusters. The coinfected prior grouping is again isolated, though one genotype evidently clusters better with the infected isolates.

Analysis of population heterozygosity

Observed heterozygosity was significantly lower than expected under Hardy–Weinberg equilibrium across all comparisons, including the complete population, clone-corrected genotypes, and the infection state subpopulations ($P < .01$; Fig. 5). This consistent deficit of heterozygosity suggests limited outcrossing both within and between infection state subpopulations.

Discussion

Saccharomyces cerevisiae is often hosting the autonomous dsRNA totivirus and its nonautonomous dsRNA satellite that when together encode the toxin-producing killer phenotype of *S. cerevisiae*, as well as the associated immunity (Schmitt and Breinig 2002, 2006). This phenomenon is well-studied under laboratory conditions (Hanes et al. 1986, Dignard et al. 1991, Marquina et al. 2002, Wickner 1996a), yet the prevalence of totivirus–satellite coinfections in natural populations is less well studied (Starmer et al. 1987, Chang et al. 2015, Boynton 2019, Travers-Cook et al. 2023). It remains unclear whether totivirus-induced proteostatic stress in the host (Chau et al. 2023), the intrinsic conflict of asymmetric dependence of satellites on totiviruses, and host sexual reproduction, disrupt what should be, based on present knowledge, a strictly vertically transmitted mycoviral infection (Taylor et al. 2014, Quintero-Blanco et al. 2022, Travers-Cook et al. 2023).

We found that approximately half of the collection was infected by a dsRNA totivirus (55.1%), whilst toxin-encoding satellites were only found to coinfect with totiviruses in a third of these isolates (37.1%). The proportion of isolates infected by totiviruses in this collection was similar to other screening studies, however coinfections were found to be considerably lower in frequency when compared to the earlier studies (Crabtree et al. 2023). However, Crabtree et al. (2023) opportunistically used *S. cerevisiae* from both human and natural sites, so a direct comparison with this paper is not possible. The proportion of yeast isolates with coinfections was found to be highly variable both across vineyards within years and between years (Fig. 1B). Such variability across vineyards in representation of each infection state demonstrates a discordance between local and regional processes governing the presence of each infection type. Yeast isolates with each of the infection states were found to represent whole vineyard-isolate sets (Fig. 1B).

Yeast isolates with totivirus–satellite coinfections experienced a major decline from 2018 into 2019, which was largely due to a single genotype (Fig. 2) experiencing local extinctions across many of the vineyards it was previously present in, as well as a near-complete extinction across all vineyards. The drivers of this genotype's disappearance are unknown, though we hypothesize that the redundancy of toxin production, when resistance emerges, may be involved (Boynton 2019, Travers-Cook et al. 2023). The overall rarity of yeast isolates harbouring the putatively advantageous toxin-encoding satellites suggests that negative frequency-dependent selection regulates their prevalence, thereby maintaining infection-state polymorphism in the population (Christie and McNickle 2023, Sica et al. 2024, Zhong et al. 2024). However, it remains to be seen whether these fluctuations can be linked to the benefits and costs of each infection state under specific ecological conditions.

The prevalence of totivirus-infected yeast isolates is a greater challenge to explain. Yeast with totivirus infections, but lacking the satellite, are expected to incur the costs of maintaining the totivirus without gaining the toxin-encoding benefits provided by the satellite (Boynton 2019, Chau et al. 2023a). Whilst intracellular selection should favour mutant totiviruses with higher virulence, selection should act against yeast with virulent totiviruses because of their reduced fitness compared to those infected by benign totiviruses. In low population density environments, the loss of the satellite may be inconsequential. However, at high population densities, when toxins are most effective as interference competition strategies (Greig and Travisano 2008), yeast with totivirus infections should be selected against. Thus, the persistence of this infection-based polymorphism is likely to depend on density-dependent processes, in which their persistence relies on low densities and minimal competition. The near-complete replacement of yeast with totivirus infections by those without infections in 2021 may be explained by the costs of totiviruses to their yeast hosts—a burden uninfected yeasts do not experience.

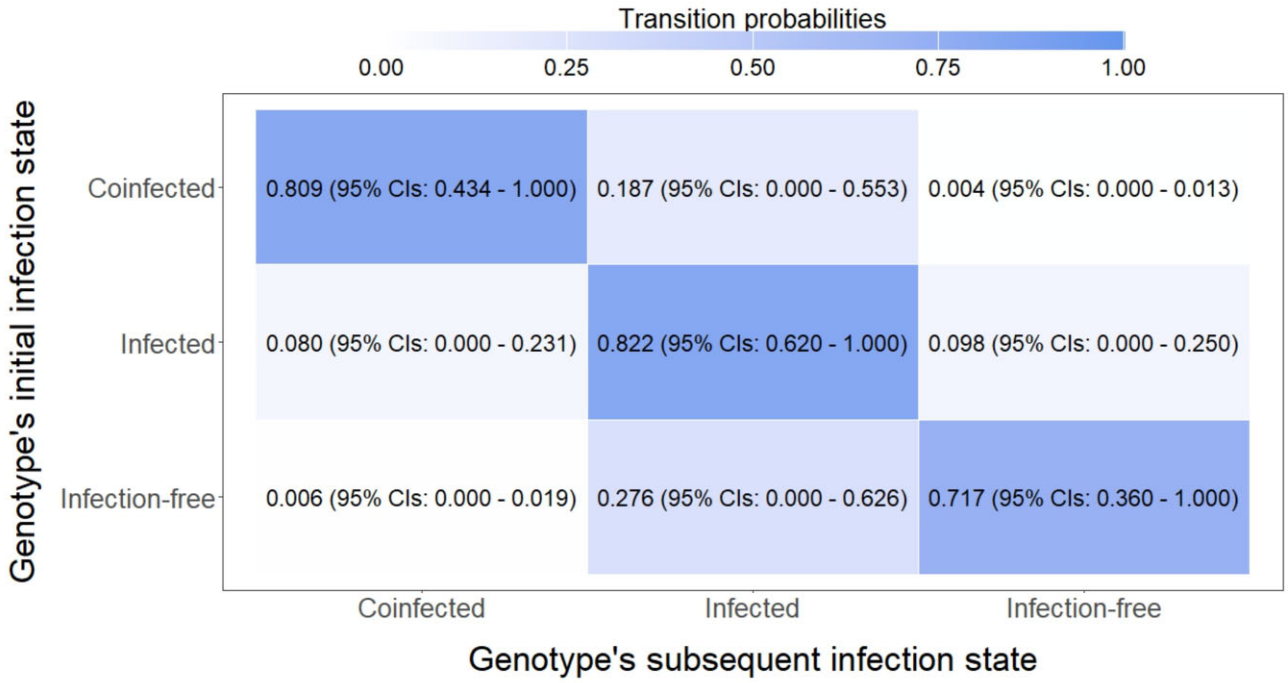

Figure 3. Transition probabilities across the infection states. Values in the centre of each cell constitute the average transition probability across all genotypes, as well as the 95% confidence intervals. Each row sums to 1; however, rounding to three decimal places introduces slight discrepancies.

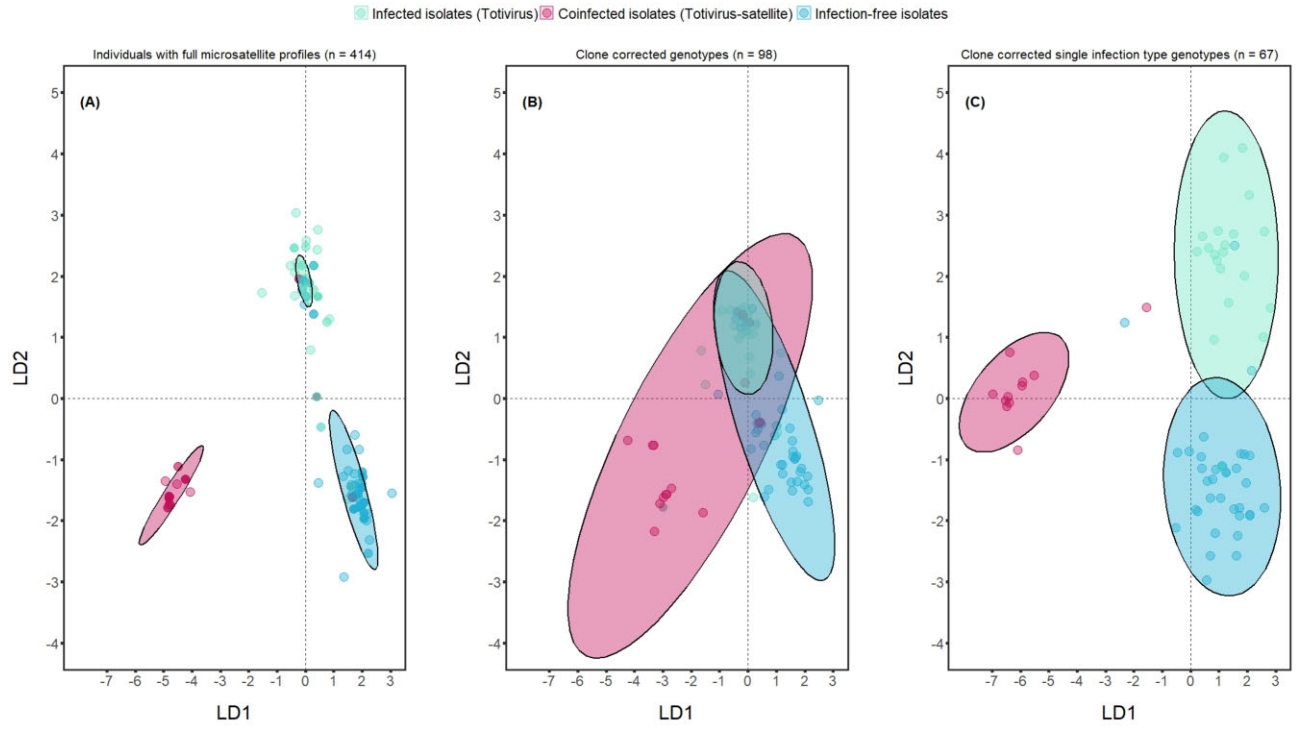

Figure 4. The two linear discriminants of the DAPC analysis using microsatellite data with viral infection status as a prior. Circles represent the individual isolates and their colour indicates the individual's infection status, whilst the infection status prior genotype space with 95% confidence intervals are represented by inertia ellipses. (A) All individual isolates that have complete microsatellite profiles after application of our conservative genotype assignment method ($n = 414$); (B) Clone corrected genotypes based on all individuals isolate that have complete microsatellite profiles, with replicates of genotypes with multiple infection states ($n = 98$); (C) Clone-corrected genotypes based on all individual's isolate that have complete microsatellite profiles, but excluding genotypes that are observed to have isolates with different infection statuses ($n = 67$).

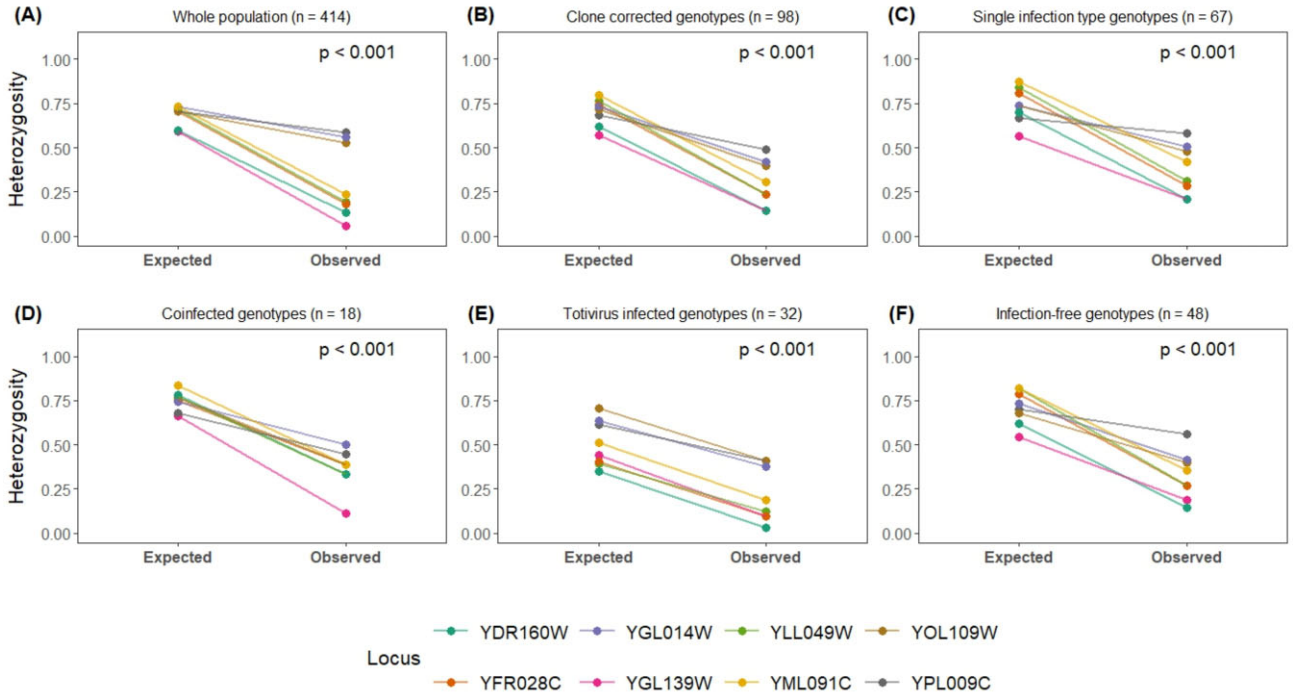

Figure 5. Expected vs. observed heterozygosity for: (A) the whole population with complete microsatellite data, (B) clone-corrected genotypes, (C) clone-corrected genotypes with single infection states, (D) totivirus–satellite coinfection genotypes, (E) totivirus-infected genotypes, and (F) uninfected genotypes.

We hypothesized that infection states would diverge alongside their host genotypes, given that *S. cerevisiae* primarily reproduces asexually, thereby linking infection state directly to host lineages. For this pattern not to emerge, frequent sexual reproduction would need to occur between genotypes with differing infection states. Such events would mix evolutionarily isolated lineages, homogenize infections, and/or decouple infection states from host lineages, ultimately disrupting the expected pattern of genotype clustering by infection state that arises from clonal reproduction. The DAPC results demonstrate that, with high MSA, we can cluster host genotypes by their infection states. This supports our hypothesis that totiviruses and the satellites primarily experience vertical transmission from parent to progeny, because genotypes that are most closely related to each other host the same infection states. As expected, this was most evident when genotype frequencies were included (Fig. 4A) and genotypes with infection state transitions are excluded (Fig. 4C), because inclusion of genotypes with multiple infection states (Fig. 4B) will give increased weighting to these genotypes.

Under a stepwise infection transition scenario, the totivirus-infected state acts as an intermediate transition state between being coinfected with both the totivirus and its satellite, and being infection-free. Our DAPC models support this scenario (Fig. 4), given that the totivirus-infection genotype cluster tended to fall within an intermediate genotype space between the coinfected and infection-free clusters. A stepwise infection state transition scenario is also supported by genotypes that were sampled across years (Fig. 3). While resampled genotypes across years most frequently maintained their infection state (Fig. 2), when they did experience infection state transitions, it was almost exclusively in a stepwise manner (Fig. 3). Though rare, these transitions indicate that yeast isolates within the same microsatellite genotype can differ in viral state, implying that totivirus and/or satellite loss can occur within the timeframe of a microsatellite genotype. Infection state transitions may have occurred prior to yeast isolates being samples, with changes instead reflecting frequency shifts driven by selection and drift. However, any changes in infection state would still have occurred recently, given the rapid evolution of microsatellites.

Removal of the satellite nucleic acid under laboratory conditions is considerably more straightforward than that of the totivirus, which we find moderate support for in this study (Fig. 2; Wickner 1974, Gao et al. 2019). The mechanisms by which *S. cerevisiae* eliminates the totivirus are largely unknown, though various mechanisms have been identified for controlling their copy number proliferation (Rowley et al. 2016, Gao et al. 2019). The only known mechanism by which these elements can be acquired is through cytoplasmic mixing during sexual reproduction. Sex and recombination should disrupt the combinations of microsatellite alleles that define genotypes, and the same genotypes would be unlikely to reappear across years. Observed heterozygosity in the population was significantly lower than expected under Hardy–Weinberg equilibrium (Fig. 5A–C), indicating that outcrossing is infrequent in the population. The strict clustering in the clone-corrected DAPC, when excluding genotypes that experienced infection state transitions (Fig. 4C), further suggests any sexual reproduction occurs primarily within infection state subpopulations. However, the significant deficit of heterozygosity within these subpopulations indicates that outcrossing is rare even at this level (Fig. 5D–F). Taken together, these results suggest that sexual transmission is unlikely to be a major driver of novel or higher-state infections.

Intragenotypic gains of totiviruses and/or satellites across years may indicate that individuals with higher infection states were already present in prior years but went undetected, indicating an issue of the sampling effort. Our results are, however, also

consistent with, and suggestive of, the possibility of extracellular acquisition of totiviruses and/or their satellites, given that genotypes can statistically acquire mycoviruses over time despite the lack of evidence for sexual reproduction. While this phenomenon has not been previously detected and is considered unlikely, because mycoviruses do not cause cell lysis (Ghabrial and Suzuki 2009, Ghabrial et al. 2015), the idea has gained support in recent years, and several mechanisms have been proposed (Buivydaite et al. 2024). This is not to imply that our results provide evidence for the extracellular acquisition of mycoviruses; rather, they are more consistent with extracellular acquisition being the mechanism for mycovirus gains, rather than sexual transmission. Given the growing interest in the possibility of extracellular acquisition of mycoviruses (Buivydaite et al. 2024), experimental approaches should be employed to test the feasibility of this phenomenon. Statistical transitions may not be evidence of transitions within the years of the dataset, but instead frequency fluctuations of infection states within genotypes as a result of selection and drift, in which gains and losses of infections occurred earlier. Given the rapid evolution of microsatellite loci, these infection state transitions are unlikely to be ancient events and more likely occurred in the recent past. Nonetheless, because the number of microsatellite loci used did not yield an asymptote in genotype richness, it remains possible that multiple closely related genotypes are being collapsed into a single detected genotype. While unlikely, some apparent intragenotypic infection-state transitions could therefore reflect cryptic sister genotypes with different infection states that are masked as one. Our findings on infection-state changes are the first reported from natural yeast populations, and given their inferred nature, warrant further exploration and verification.

Transitions occur frequently within genotypes (Figs 2 and 3), yet clustering by infection state is still apparent across genotypes (Fig. 4C). At the same time, the presence of multiple infection states within a single genotype disrupts the clustering of host genotypes by infection status (Fig. 4B). This apparent contradiction can be explained if each host genotype has an optimal infection state: offspring that transition away from this state are less fit over time, allowing the original infection-state clustering to be maintained at the population level. There is extensive literature on host genes affecting the maintenance of dsRNAs in *S. cerevisiae* (Magliani et al. 1997, Wickner 1996a, b). Recessive mutations in a number of *mak* genes have been shown to result in the loss of the satellite during haploid stages (Magliani et al. 1997). In many cases, the totivirus remains unaffected by these recessive mutants whilst the satellite is eliminated (*MAK4*, *MAK5*, *MAK6*, *MAK7*, *MAK14*, and *MAK15*) (Wickner and Leibowitz 1976, 1979, Magliani et al. 1997). Three genes (*MAK3*, *MAK10*, and *PET18*) are known to be necessary for the maintenance of totiviruses as well as their satellites (Fujimura et al. 1986, Fujimura and Wickner 1987, Schmitt and Tipper 1992, Tercero and Wickner 1992, Tercero et al. 1993). Tracking variants in genes involved in infection maintenance could provide insight into the causes of transitions, as well as the factors influencing their persistence or suboptimality.

We report the persistence of infection-based competitive polymorphism in a natural population of *S. cerevisiae*. We demonstrate that infection state divergence occurs with host genotypes, and that transitions in infection type are also occurring over short time scales. However, transitions to suboptimal infection types are unlikely to persist over longer periods as they would disrupt the clustering of host genotypes by infection types. The results of our study underscore the need for more resolute longitudinal studies, both intraseasonal and interannual, to investigate the dynamics of infection-based competitive polymorphism in the killer yeast system. Such studies should integrate host genomics, infection dynamics, and both competition and fitness assays.

Acknowledgements

The authors would like to thank two anonymous reviewers whose feedback during the review process vastly improved this manuscript.

Author contributions

Tommy J. Travers Cook (Conceptualization, Data curation, Formal Analysis, Investigation, Methodology, Project administration, Validation, Visualization, Writing – original draft, Writing – review & editing), Sarah J. Knight (Data curation, Funding acquisition, Methodology, Resources), Soon A. Lee (Data curation, Writing – review & editing), Jana Jucker (Investigation, Writing – review & editing), Tamara Schlegel (Data curation, Writing – review & editing), Jukka Jokela (Conceptualization, Supervision, Writing – review & editing), Claudia C. Buser (Conceptualization, Funding acquisition, Resources, Supervision, Writing – review & editing).

Supplementary data

Supplementary data are available at *FEMSEC Journal* online.

Conflict of interest: None declared.

Funding

This project was funded the ETH Zurich research grant, ETH-23 20-1.

References

Alizon S, Hurford A, Mideo N *et al*. Virulence evolution and the trade-off hypothesis: history, current state of affairs and the future. *J Evol Biol* 2009;**22**:245–59. https://doi.org/10.1111/j.1420-9101.2008.01658.x.

Anderson RM, May RM. Coevolution of hosts and parasites. *Parasitology* 1982;**85**:411–26. https://doi.org/10.1017/s0031182000055360.

Bennett RJ, Turgeon BG. Fungal sex: the ascomycota. *Microbiol Spectr* 2016;**4**. https://doi.org/10.1128/microbiolspec.FUNK-0005-2016.

Bostian KA, Sturgeon JA, Tipper DJ. Encapsidation of yeast killer double-stranded ribonucleic acids: dependence of M on L. *J Bacteriol* 1980;**143**:463–70. https://doi.org/10.1128/jb.143.1.463-470.1980.

Boynton PJ. The ecology of killer yeasts: interference competition in natural habitats. *Yeast* 2019;**36**:473–85. https://doi.org/10.1002/yea.3398.

Bronstein JL. Conditional outcomes in mutualistic interactions. *Trends Ecol Evol* 1994;**9**:214–7. https://doi.org/10.1016/0169-5347(94)90246-1.

Buivydaite Z, Winding A, Sapkota R. Transmission of mycoviruses: new possibilities. *Front Microbiol* 2024;**15**:1432840. https://doi.org/10.3389/fmicb.2024.1432840.

Bull JJ. Virulence. *Evolution* 1994;**48**:1423–37. https://doi.org/10.1111/j.1558-5646.1994.tb02185.x.

Bürkner PC. brms: an R package for bayesian multilevel models using Stan. *J Stat Soft* 2017;**80**:1–28. https://doi.org/10.18637/jss.v080.i01.

Chang SL, Leu JY, Chang TH. A population study of killer viruses reveals different evolutionary histories of two closely related

yeasts. *Mol Ecol* 2015;**24**:4312–22. https://doi.org/10.1111/mec.13310.

Chao A, Gotelli NJ, Hsieh TC *et al.* Rarefaction and extrapolation with Hill numbers: a framework for sampling and estimation in species diversity studies. *Ecol Monogr* 2014;**84**:45–67. https://doi.org/10.1890/13-0133.1.

Chau S, Gao J, Diao AJ *et al.* Diverse yeast antiviral systems prevent lethal pathogenesis caused by the L-A mycovirus. *Proc Natl Acad Sci USA* 2023;**120**:e2208695120. https://doi.org/10.1073/pnas.2208695120.

Christie MR, McNickle GG. Negative frequency dependent selection unites ecology and evolution. *Ecol Evol* 2023;**13**:e10327. https://doi.org/10.1002/ece3.10327.

Crabtree AM, Kizer EA, Hunter SS *et al.* A rapid method for sequencing double-stranded RNAs purified from yeasts and the identification of a potent K1 killer toxin isolated from *Saccharomyces cerevisiae*. *Viruses-Basel* 2019;**11**. https://doi.org/ARTN10.3390/v11010070.

Crabtree AM, Taggart NT, Lee MD *et al.* The prevalence of killer yeasts and double-stranded RNAs in the budding yeast. *FEMS Yeast Res* 2023;**23**. https://doi.org/ARTNfoad05110.1093/femsyr/foad051.

de Melo Pereira GV, Ramos CL, Galvao C *et al.* Use of specific PCR primers to identify three important industrial species of *Saccharomyces* genus: *Saccharomyces cerevisiae* , *Saccharomyces bayanus* and *Saccharomyces pastorianus*. *Lett Appl Microbiol* 2010;**51**:131–137. https://doi.org/10.1111/j.1472-765X.2010.02868.x.

Dignard D, Whiteway M, Germain D *et al.* Expression in yeast of a cDNA copy of the K2 killer toxin gene. *Molec Gen Genet* 1991;**227**:127–36. https://doi.org/10.1007/BF00260717.

Dinman JD, Icho T, Wickner RB. A-1 ribosomal frameshift in a double-stranded RNA virus of yeast forms a gag-pol fusion protein. *Proc Natl Acad Sci USA* 1991;**88**:174–8. https://doi.org/10.1073/pnas.88.1.174.

Dinman JD, Wickner RB. Translational maintenance of frame: mutants of *Saccharomyces cerevisiae* with altered -1 ribosomal frameshifting efficiencies. *Genetics* 1994;**136**:75–86. https://doi.org/10.1093/genetics/136.1.75.

Doebeli M, Knowlton N. The evolution of interspecific mutualisms. *Proc Natl Acad Sci USA* 1998;**95**:8676–80. https://doi.org/10.1073/pnas.95.15.8676.

Douma JC, Weedon JT. Analysing continuous proportions in ecology and evolution: a practical introduction to beta and dirichlet regression. *Methods Ecol Evol* 2019;**10**:1412–30. https://doi.org/10.1111/2041-210x.13234.

El Haloui N, Picque D, Corrieu G. Alcoholic fermentation in winemaking: on-line measurement of density and carbon dioxide evolution. *J Food Eng* 1988;**8**:17–30. https://doi.org/https://doi.org/10.1016/0260-8774(88)90033-7.

Ewald PW. Transmission modes and evolution of the parasitism-mutualism continuum. *Ann NY Acad Sci* 1987;**503**:295–306. https://doi.org/10.1111/j.1749-6632.1987.tb40616.x.

Fujimura T, Esteban R, Wickner RB. In vitro L-A double-stranded RNA synthesis in virus-like particles from *Saccharomyces cerevisiae*. *Proc Natl Acad Sci USA* 1986;**83**:4433–7. https://doi.org/10.1073/pnas.83.12.4433.

Fujimura T, Ribas JC, Makhov AM *et al.* Pol of gag-pol fusion protein required for encapsidation of viral RNA of yeast L-A virus. *Nature* 1992;**359**:746–9. https://doi.org/10.1038/359746a0.

Fujimura T, Wickner RB. L-A double-stranded RNA virus-like particle replication cycle in *Saccharomyces cerevisiae*: particle maturation in vitro and effects of mak10 and pet18 mutations. *Mol Cell Biol* 1987;**7**:420–6. https://doi.org/10.1128/mcb.7.1.420-426.1987.

Gao J, Chau S, Chowdhury F *et al.* Meiotic viral attenuation through an ancestral apoptotic pathway. *Proc Natl Acad Sci USA* 2019;**116**:16454–62. https://doi.org/10.1073/pnas.1900751116.

Ghabrial SA, Caston JR, Jiang D *et al.* 50-plus years of fungal viruses. *Virology* 2015;**479-480**:356–68. https://doi.org/10.1016/j.virol.2015.02.034.

Ghabrial SA, Suzuki N. Viruses of plant pathogenic fungi. *Annu Rev Phytopathol* 2009;**47**:353–84. https://doi.org/10.1146/annurev-phyto-080508-081932.

Goker M, Scheuner C, Klenk HP *et al.* Codivergence of mycoviruses with their hosts. *PLoS One* 2011;**6**:e22252. https://doi.org/10.1371/journal.pone.0022252.

Greig D, Travisano M. Density-dependent effects on allelopathic interactions in yeast. *Evolution* 2008;**62**:521–7. https://doi.org/10.1111/j.1558-5646.2007.00292.x.

Hanes SD, Burn VE, Sturley SL *et al.* Expression of a cDNA derived from the yeast killer preprotoxin gene: implications for processing and immunity. *Proc Natl Acad Sci USA* 1986;**83**:1675–9. https://doi.org/10.1073/pnas.83.6.1675.

Herre EA, Knowlton N, Mueller UG *et al.* The evolution of mutualisms: exploring the paths between conflict and cooperation. *Trends Ecol Evol* 1999;**14**:49–53. https://doi.org/10.1016/s0169-5347(98)01529-8.

,Hsieh T. C, ,Ma K., ,Chao A. iNEXT: an R package for rarefaction and extrapolation of species diversity (H ill numbers). *Methods in ecology and evolution* 2016;**7**:1451–1456. https://doi.org/10.1111/2041-210X.12613

Icho T, Wickner RB. The double-stranded RNA genome of yeast virus L-A encodes its own putative RNA polymerase by fusing two open reading frames. *J Biol Chem* 1989;**264**:6716–23. https://www.ncbi.nlm.nih.gov/pubmed/2651431.

Jombart T, Devillard S, Balloux F. Discriminant analysis of principal components: a new method for the analysis of genetically structured populations. *BMC Genet* 2010;**11**:94. https://doi.org/10.1186/1471-2156-11-94.

Jurenas D, Fraikin N, Goormaghtigh F *et al.* Biology and evolution of bacterial toxin-antitoxin systems. *Nat Rev Microbiol* 2022;**20**:335–50. https://doi.org/10.1038/s41579-021-00661-1.

Kast A, Voges R, Schroth M *et al.* Autoselection of cytoplasmic yeast virus like elements encoding toxin/antitoxin systems involves a nuclear barrier for immunity gene expression. *PLoS Genet* 2015;**11**:e1005005. https://doi.org/10.1371/journal.pgen.1005005.

Luksa J, Ravoityte B, Konovalovas A *et al.* Different metabolic pathways are involved in response of *Saccharomyces cerevisiae* to L-A and M viruses. *Toxins* 2017;**9**:233. https://doi.org/10.3390/toxins9080233.

Magliani W, Conti S, Gerloni M *et al.* Yeast killer systems. *Clin Microbiol Rev* 1997;**10**:369–400. https://doi.org/10.1128/Cmr.10.3.369.

Marquina D, Santos A, Peinado JM. Biology of killer yeasts. *Int Microbiol* 2002;**5**:65–71. https://doi.org/10.1007/s10123-002-0066-z.

McBride RC, Boucher N, Park DS *et al.* Yeast response to LA virus indicates coadapted global gene expression during mycoviral infection. *FEMS Yeast Res* 2013;**13**:162–79. https://doi.org/10.1111/1567-1364.12019.

Messenger SL, Molineux IJ, Bull JJ. Virulence evolution in a virus obeys a trade-off. *Proc R Soc Lond B* 1999;**266**:397–404. https://doi.org/10.1098/rspb.1999.0651.

Nadai C, Bovo B, Giacomini A *et al.* New rapid PCR protocol based on high-resolution melting analysis to identify *Saccharomyces cerevisiae* and other species within its genus. *J Appl Microbiol* 2018;**124**:1232–42. https://doi.org/10.1111/jam.13709.

Nieuwenhuis BP, James TY. The frequency of sex in fungi. *Phil Trans R Soc B* 2016;**371**. https://doi.org/10.1098/rstb.2015.0540.

Pereira GMD, Ramos CL, Galvao C *et al.* Use of specific PCR primers to identify three important industrial species of *Saccharomyces* genus: *Saccharomyces cerevisiae* , *Saccharomyces bayanus* and *Saccharomyces pastorianus*. *Lett Appl Microbiol* 2010;**51**:131–7. https://doi.org/10.1111/j.1472-765X.2010.02868.x.

Pieczynska MD, de Visser JA, Korona R. Incidence of symbiotic dsRNA 'killer' viruses in wild and domesticated yeast. *FEMS Yeast Res* 2013;**13**:856–9. https://doi.org/10.1111/1567-1364.12086.

Pieczynska MD, Korona R, De Visser JAG. Experimental tests of host–virus coevolution in natural killer yeast strains. *J Evol Biol* 2017;**30**:773–81. https://doi.org/10.1111/jeb.13044.

Quintero-Blanco J, Delodi E, Garzón A *et al.* Sexually-driven combinatorial diversity in native *Saccharomyces* wine yeasts. *Fermentation* 2022;**8**:569. https://doi.org/https://doi.org/10.3390/fermentation8100569.

R Core Team. *R: A Language and Environment for Statistical Computing*. Vienna: R Foundation for Statistical Computing, 2023. https://www.R-project.org. Last accessed 1.12. 2025.

Richards KD, Goddard MR, Gardner RC. A database of microsatellite genotypes for *Saccharomyces cerevisiae*. *Antonie Van Leeuwenhoek* 2009;**96**:355–9. https://doi.org/10.1007/s10482-009-9346-3.

Rowley PA, Ho B, Bushong S *et al.* XRN1 is a species-specific virus restriction factor in yeasts. *PLoS Pathog* 2016;**12**:e1005890. https://doi.org/10.1371/journal.ppat.1005890.

Sachs JL, Essenberg CJ, Turcotte MM. New paradigms for the evolution of beneficial infections. *Trends Ecol Evol* 2011;**26**:202–9. https://doi.org/10.1016/j.tree.2011.01.010.

Schmitt MJ, Breinig F. The viral killer system in yeast: from molecular biology to application. *FEMS Microbiol Rev* 2002;**26**:257–76. https://doi.org/PIIS0168-6445(02)00099-2. doi:10.1111/j.1574-6976.2002.tb00614.x.

Schmitt MJ, Breinig F. Yeast viral killer toxins: lethality and self- protection. *Nat Rev Microbiol* 2006;**4**:212–21. https://doi.org/10.1038/nrmicro1347.

Schmitt MJ, Tipper DJ. Genetic analysis of maintenance and expression of L and M double-stranded RNAs from yeast killer virus K28. *Yeast* 1992;**8**:373–84. https://doi.org/10.1002/yea.320080505.

Schmitt MJ, Tipper DJ. Sequence of the M28 dsRNA: preprotoxin is processed to an alpha/beta heterodimeric protein toxin. *Virology* 1995;**213**:341–51. https://doi.org/10.1006/viro.1995.0007.

Sica J, Vendramini C, Nadai C *et al.* Strain prevalence and killer factor only partially influence the fermentation activity of pairwise *Saccharomyces cerevisiae* wine strains inoculation. *PLoS One* 2024;**19**:e0300212. https://doi.org/10.1371/journal.pone.0300212.

Starmer WT, Ganter PF, Aberdeen V *et al.* The ecological role of kiler yeasts in natural communities of yeasts. *Can J Microbiol* 1987;**33**:783–96. https://doi.org/10.1139/m87-134.

Taylor BP, Cortez MH, Weitz JS. The virus of my virus is my friend: ecological effects of virophage with alternative modes of coinfection. *J Theor Biol* 2014;**354**:124–36. https://doi.org/10.1016/j.jtbi.2014.03.008.

Tercero JC, Dinman JD, Wickner RB. Yeast MAK3 N- acetyltransferase recognizes the N-terminal four amino acids of the major coat protein (gag) of the L-A double-stranded RNA virus. *J Bacteriol* 1993;**175**:3192–4. https://doi.org/10.1128/jb.175.10.3192-3194.1993.

Tercero JC, Wickner RB. MAK3 encodes an N-acetyltransferase whose modification of the L-A gag NH2 terminus is necessary for virus particle assembly. *J Biol Chem* 1992;**267**:20277–81. https://www.ncbi.nlm.nih.gov/pubmed/1400344.

Travers-Cook TJ, Jokela J, Buser CC. The evolutionary ecology of fungal killer phenotypes. *Proc R Soc B Biol Sci* 2023;**290**. https://doi.org/ARTN2023110810.1098/rspb.2023.1108.

Wickham H. ggplot2. *WIREs Comput Stat* 2011;**3**:180–5. https://doi.org/10.1002/wics.147.

Wickner RB, Edskes HK. Yeast killer elements hold their hosts hostage. *PLoS Genet* 2015;**11**:e1005139. https://doi.org/10.1371/journal.pgen.1005139.

Wickner RB, Fujimura T, Esteban R. Viruses and prions of *Saccharomyces cerevisiae*. *Adv Virus Res* 2013;**86**:1–36. https://doi.org/10.1016/B978-0-12-394315-6.00001-5.

Wickner RB, Leibowitz MJ. Chromosomal genes essential for replication of a double-stranded RNA plasmid of *Saccharomyces cerevisiae*: the killer character of yeast. *J Mol Biol* 1976;**105**:427–43. https://doi.org/10.1016/0022-2836(76)90102-9.

Wickner RB, Leibowitz MJ. Mak mutants of yeast: mapping and characterization. *J Bacteriol* 1979;**140**:154–60. https://doi.org/10.1128/jb.140.1.154-160.1979.

Wickner RB. "Killer character" of *Saccharomyces cerevisiae*: curing by growth at elevated temperature. *J Bacteriol* 1974;**117**:1356–7. https://doi.org/10.1128/jb.117.3.1356-1357.1974.

Wickner RB. Double-stranded RNA viruses of *Saccharomyces cerevisiae*. *Microbiol Rev* 1996a;**60**:250–65. https://doi.org/10.1128/mr.60.1.250-265.1996.

Wickner RB. Prions and RNA viruses of *Saccharomyces cerevisiae*. *Annu Rev Genet* 1996b;**30**:109–39. https://doi.org/10.1146/annurev.genet.30.1.109.

Woods DR, Bevan EA. Studies on the nature of the killer factor produced by *Saccharomyces cerevisiae*. *J Gen Microbiol* 1968;**51**:115–26. https://doi.org/10.1099/00221287-51-1-115.

Zhong V, Ketchum N, Mackenzie JK *et al.* Inhibition of diastatic yeasts by *Saccharomyces* killer toxins to prevent hyperattenuation during brewing. *Appl Environ Microbiol* 2024;**90**:e0107224. https://doi.org/10.1128/aem.01072-.

Received 5 May 2025; **revised** 17 November 2025; **accepted** 17 November 2025